Chapter 5

THE MODULE FOR DETERMINING AN OBJECT'S *TRUE* GRAY LEVELS

This chapter discusses the module for determining an object's *true* gray levels. To compute the *true* gray levels of an object of interest requires the removal of the overlapping background effects. This problem is quite complex and takes several steps to be resolved. First in Section 5.1, it will be shown that an *n*-object-overlapping problem can always be simplified to a two-object-overlapping problem. So the research focus turns to computing *true* gray levels for two-object-overlapping problem. Since there is no existing method for accomplishing this task in either the transmission or the scatter image modalities, it was necessary to develop models that can be used to remove the background object overlapping effects. Section 5.2 discusses the development of the mathematical models for removing the overlapping effects for the transmission modalities. Section 5.3 discusses the models for the forward-scatter modality. Section 5.4 discusses the models for the backscatter modality and summarizes the mathematical model development. In luggage inspection, it is difficult to identify the correct object that is overlapped with the object of interest. Section 5.5 analyzes the luggage inspection problem, and gives an algorithm that determines the *true* gray level of an object of interest in the luggage environment. Section 5.6 concludes this chapter. This chapter documents this research work, which is a unique contribution to the explosive detection community.

5.1 The Basic Method for Removing Overlapping Effects

This section begins by illustrating the method for determining the *true* gray level of an object of interest when it only overlaps with another object. It will show that an *n*-object-overlapping problem can always be simplified to a two-object-overlapping problem. So being able to determine the *true* gray level in a two-object-overlapping problem means the ability to determine the *true* gray level in any overlapping problem.

Figure 5.1-1 illustrates the method for determining the *true* gray level in a two-object-overlapping problem. In this figure, several symbols are used. Symbol *Obj* refers to an object. Obj_1 is the object of interest, and Obj_2 is the background object that overlaps with Obj_1. Symbol *Rgn* refers to a region in an x-ray image. Rgn_1 is a region uniquely formed by Obj_1; Rgn_2 is a region uniquely formed by Obj_2; and Rgn_3 is the region formed by Obj_1 overlapping with Obj_2. Please note that "gray level" is used in singular form because the discussion here assumes to be in one sensing modality rather than in all four sensing modalities. Also the segmentation algorithm has segmented an image into regions with relatively uniform gray levels. Thus each region can be characterized using its average gray level.

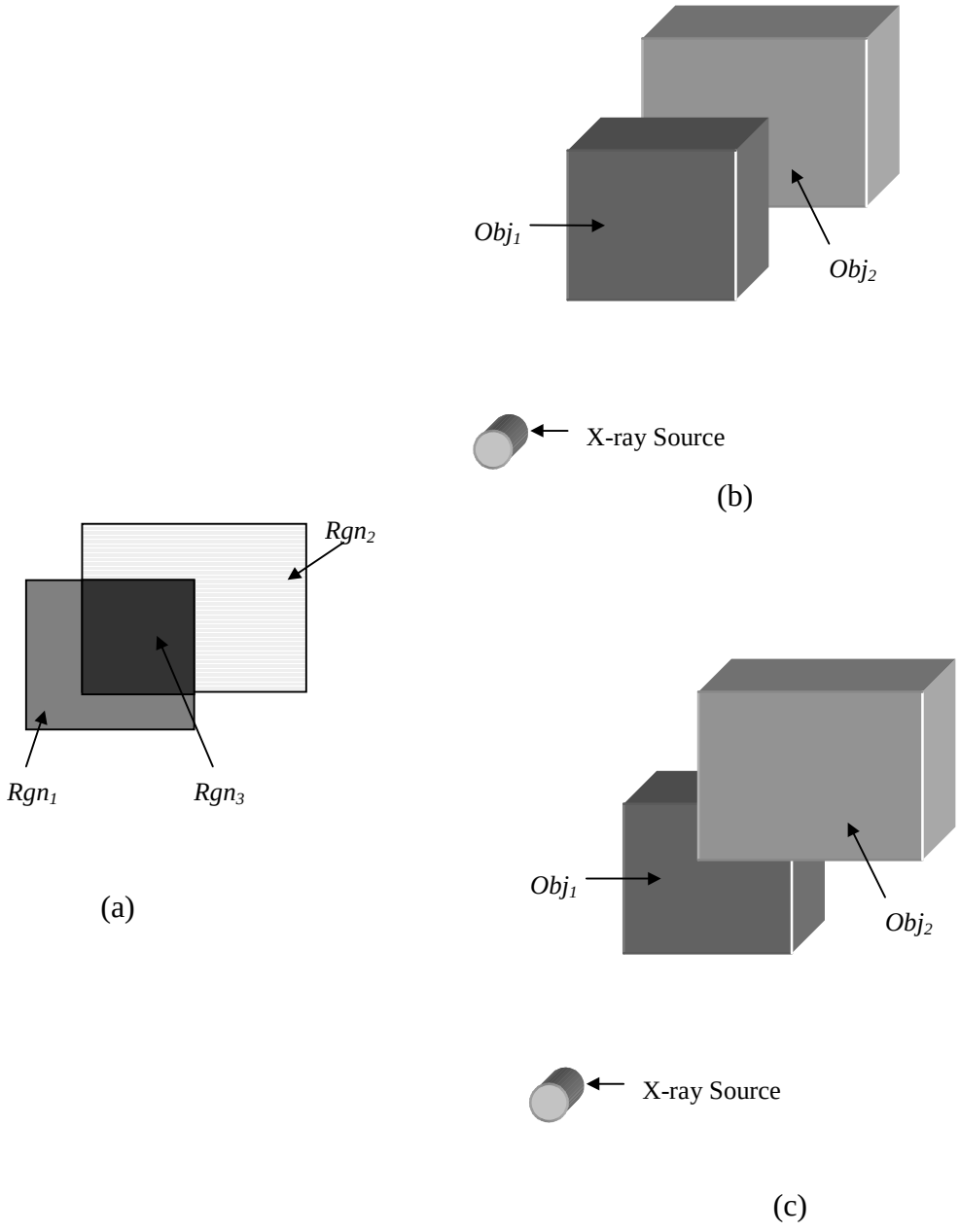

Figure 5.1-1 Illustration of two-object-overlapping scenarios. a) Three regions are formed in the projected x-ray image. Rgn_1 and Rgn_2 are formed by Obj_1 and Obj_2 respectively. Rgn_3 is formed by Obj_1 overlapping with Obj_2. b) Obj_1 may be in front of Obj_2. c) Obj_1 may be behind of Obj_2.

The average gray level of Rgn_1 is the *true* gray level of Obj_1. A typical two-object-overlapping scenario is that Rgn_1 does not appear in an image, and only the overlapped region Rgn_3 and the background object region Rgn_2 appear. Thus the average gray level of Rgn_1 cannot be directly measured. Fortunately there is a fixed relationship between the gray level of Rgn_3 and the *true* gray levels of Obj_1 and Obj_2. From Section 5.2 to Section 5.4 mathematical equations are established to model this relationship for the different sensing modalities. Those mathematical equations are called overlap models. Each model allows the computation of the gray level of the overlapped region Rgn_3 in an imaging modality using the *true* gray levels of Obj_1 and Obj_2. Most importantly, each model, after careful manipulation, also allows the computation of the *true* gray level of Obj_1 once the gray level of Rgn_3 and the *true* gray level of Obj_2 are known. Using these models, the overlapping effects are removed from the object of interest, and the *true* gray levels can be computed for the object of interest in all four sensing modalities.

Due to x-ray physics, the relative positions of Obj_1 to Obj_2 makes no difference in the transmission modality. It does make difference in the either scatter modality. So there should be one model for low-energy transmission modality; one model for high-energy transmission modality; two models for forward scatter modality; and two models for backscatter modality.

To understand that all overlapping problems can be simplified to a two-object-overlapping problem, first, a three-object-overlapping problem is examined. Assume that three objects are overlapped as seen in Figure 5.1-2. Since Rgn_2 is formed by Obj_2 overlaps with Obj_3, Obj_2 and Obj_3 together can be viewed as one pseudo-object Obj_2' rather than two separate objects. This pseudo-object overlaps with Obj_1, and it also forms a neighboring region Rgn_2. The *true* gray level of Obj_2' can be ***directly*** measured at region Rgn_2 without the knowledge of *true* gray levels from either Obj_2 or Obj_3. Since the image region Rgn_1 is formed by Obj_1 overlapped Obj_2', by removing the overlapping effects caused by Obj_2', the *true* gray level of Obj_1 is revealed. The three-object-overlapping problem is thus simplified to a two-object-overlapping problem.

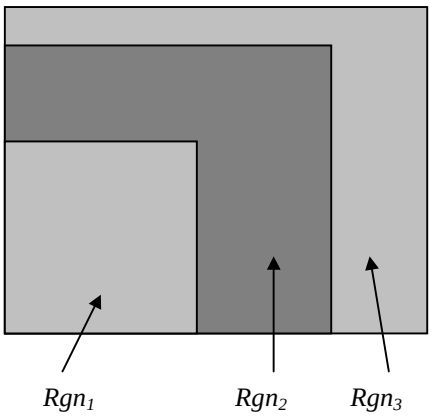

(a)

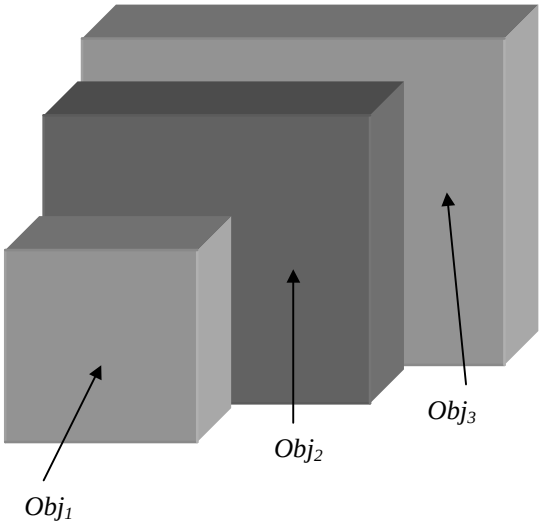

(b)

Figure 5.1-2 Illustration of a three-object-overlapping problem. a) The image regions that are formed by three overlapped objects. b) The three objects that are overlapped.

The simplification procedure is generally true for any *n*-object-overlapping problem. When an object of interest is overlapped with *(n-1)* objects, those *(n-1)* objects can always be considered as one pseudo-object. The *true* gray level of this pseudo-object can always be measured from one of the neighboring regions. By removing the overlapping effect caused by this pseudo-object, the *true* gray level of the object of interest is revealed. The *n*-object-overlapping problem is thus simplified to a two-object-overlapping problem.

5.2 Transmission Overlap Models

In general, the method for developing an overlap mathematical model for a certain sensing modality is as follows. First, a mathematical model is established to formulate the overlapping relationship. Each mathematical model contains undefined constants. A number of overlapping experiments was designed to obtain the data that can later be used to define values for those constants. Note that the physical interactions that are occurring can be quite complex. However, the purpose for the model development is to compute *true* gray levels of object of interest in real-time. Consequently each model must be mathematically simple.

Before getting into the discussion of the development of the low-energy transmission overlap model, it is important to know the relationship between the x-ray signal intensity and image gray level. All the x-ray physics analysis that is used to establish the overlap models is in terms of x-ray beam intensity. However, the AS&E system can only collect x-ray images that are in terms of pixel gray levels. In order to find the values for the constants in those mathematical models, gray levels must be converted to x-ray intensities. In order to use the overlap models to compute the *true* gray levels of an object of interest, the models must be converted into equations that are in terms of gray levels.

In Section 3.3 it was found that image gray level is a linear function of x-ray signal intensity:

$$g = cI \tag{3.3-6}$$

where g is the gray level of a pixel, I is the x-ray beam intensity, and c is a conversion constant. The value of c is different for different sensing modalities. So for different sensing modalities:

$$g^H = c^H I^H \tag{5.2-1}$$

$$g^L = c^L I^L \tag{5.2-2}$$

$$g^F = c^F I^F \tag{5.2-3}$$

$$g^B = c^B I^B \tag{5.2-4}$$

where c^H, c^L, c^F, and c^B are the conversion constants for high-energy transmission, low-energy transmission, forward scatter, and backscatter modalities respectively. Those constants need not to be solved, because they are eventually canceled out in the derivation. Also, in transmission modalities, the gray level of an incident x-ray beam is 255, thus:

$$c^H I_0^H = 255 \tag{5.2-5}$$

$$c^L I_0^L = 255 \tag{5.2-6}$$

where I_0^H and I_0^L are the intensity of the high- and low-energy incident x-ray beams respectively.

In low-energy transmission modality, when the incident x-ray beam I_0^L traverses through an object, its intensity I^L is reduced to:

$$I^L = I_0^L e^{-\sigma m x} \tag{5.2-7}$$

The attenuation coefficient $e^{-\sigma nx}$ of this object is computed as:

$$e^{-\sigma nx} = I^L / I_0^L \tag{5.2-8}$$

Let us examine the two-object-overlapping problem as seen in Figure 5.1-1. For convenience, denote the overlapped region as *Rgn*, and its x-ray intensity as I_{Rgn}^L. The attenuation coefficients of Obj_1 and Obj_2 are $e^{-\sigma_1 n_1 x_1}$ and $e^{-\sigma_2 n_2 x_2}$ respectively. The x-ray intensity at the overlapped region *Rgn* can be computed as:

$$I_{Rgn}^L = I_0^L e^{-\sigma_1 n_1 x_1} e^{-\sigma_2 n_2 x_2} \tag{5.2-9}$$

The attenuation coefficient $e^{-\sigma_1 n_1 x_1}$ can be computed as I_1^L / I_0^L, and $e^{-\sigma_2 n_2 x_2}$ can be computed as I_2^L / I_0^L, where I_1^L is the x-ray intensity after I_0^L interacts with Obj_1, and I_2^L is the x-ray intensity after I_0^L interacts with Obj_2. So the x-ray intensity at the overlapped region *Rgn* can also be written as

$$I_{Rgn}^L = I_0^L \left(I_1^L / I_0^L \right) \left(I_2^L / I_0^L \right) \tag{5.2-10}$$

Since x-ray intensities cannot be directly measured but gray levels can, the above equation must be converted to a form for gray levels. So g_{Rgn}^L the gray level of region *Rgn* becomes

$$\begin{aligned} g_{Rgn}^L &= c^L I_{Rgn}^L \\ &= c^L I_0^L e^{-\sigma_1 n_1 x_1} e^{-\sigma_2 n_2 x_2} \\ &= c^L I_0^L \left(I_1^L / I_0^L \right) \left(I_2^L / I_0^L \right) \\ &= c^L I_0^L \left(c^L I_1^L / c^L I_0^L \right) \left(c^L I_2^L / c^L I_0^L \right) \\ &= \frac{\left(c^L I_1^L \right) \left(c^L I_2^L \right)}{c^L I_0^L} \\ &= \frac{g_1^L g_2^L}{255} \end{aligned} \tag{5.2-11}$$

where g_1^L and g_2^L are the *true* gray levels of Obj_1 and Obj_2 respectively. This equation establishes the relationship between the gray level of the overlapped region *Rgn* and the *true* gray levels of objects that form this region. Knowing the *true* gray levels of the objects, the gray level of the overlapped region can be computed. Knowing the gray level of the overlapped region *Rgn* and the *true* gray level of one of the object, the *true* gray level of another object can be computed.

Equation 5.2-11 is derived under the assumption that the x-ray source is a monochromatic source. However the x-ray source of AS&E system is polychromatic. To account for the polychromatic x-ray source spectrum, a constant a^L is added to Equation 5.2-11. The modified equation becomes:

$$g_{Rgn}^L = a^L \frac{g_1^L g_2^L}{255} \tag{5.2-12}$$

Constant a^L is then computed using experimental data. Experimental data are collected from three step wedges – a clear plastic step wedge, an alumni step wedge, and a white plastic step wedge.

A step wedge is shown at the top part of Figure 5.2-1. Each step is treated as an individual object. The average gray level is computed for each step in order to remove the noise in the image. Table 5.2-1 lists the thickness of each step for each step wedge. Table 5.2-2 lists the average gray levels of each step. Assume the step wedge shown in Figure 5.2-1 is a clear plastic step wedge. The thickness of step 1 is 0.6 cm; the thickness of step 3 is 1.8 cm; and the thickness of step 4 is 2.4 cm. If step 1 is considered as Obj_1, step 3 is considered as Obj_2, then step 4 can be considered as the overlapped object formed by Obj_1 and Obj_2. This is because the thickness of step 4 is equal to the thickness of step 1 plus the thickness of step 3, and step 4 is made of the same material as step 1 and 3. So by measuring the gray levels of step 1, 3, and 4, g_1^L, g_2^L, and g_{Rgn}^L can be measured.

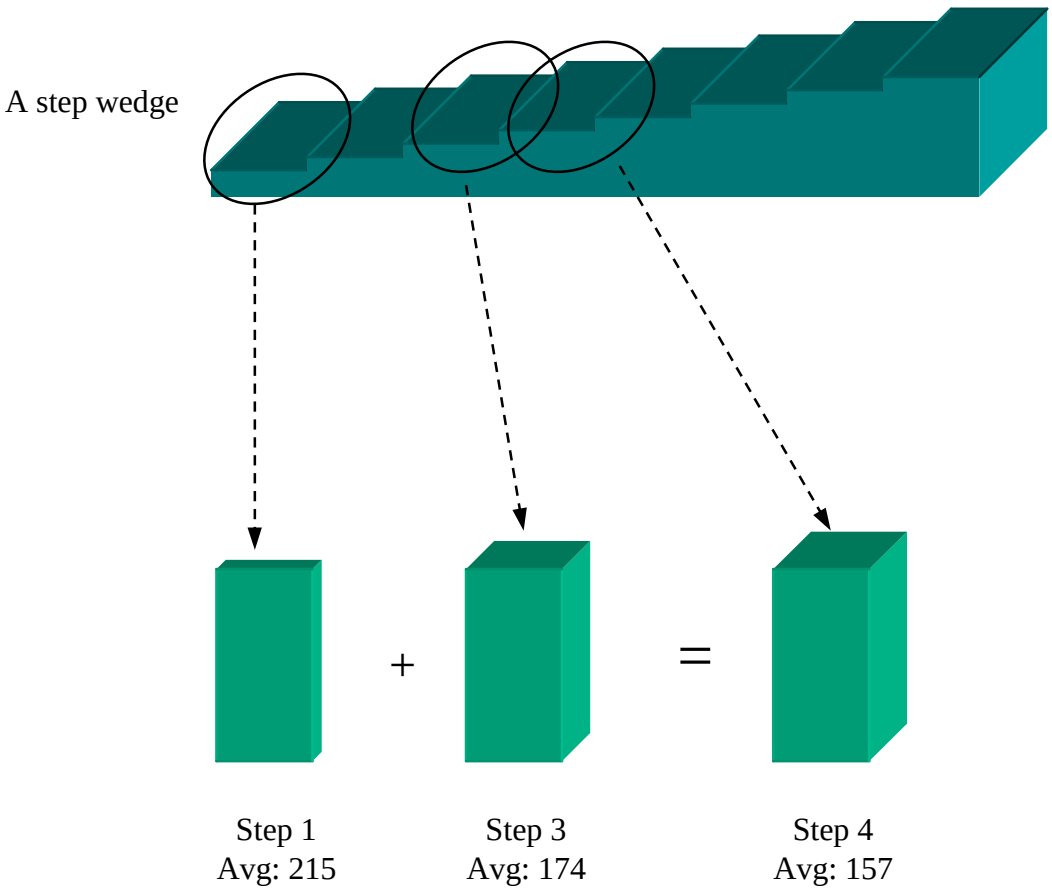

Figure 5.2-1 Illustration of data collection from a step wedge.

Table 5.2-1 Thickness of each step of each step wedge

Step Number	1	2	3	4	5	6	7	8
Clear Plastics (cm)	0.6	1.2	1.8	2.4	3.0	3.6	4.2	4.8
White Plastics (cm)	1.0	1.5	2.1	5.2	10.25	15.3	17.8	25.4
Aluminium (cm)	0.3	0.5	0.7	1.0	1.2	1.4	1.5	2.0

Table 5.2-2 *True* gray levels of steps in low-energy transmission modality

Step Number	1	2	3	4	5	6	7	8
Clear Plastics	215	192	174	157	143	129	116	106
White Plastics	164	127	108	86	76	63	63	43
Aluminium	224	203	184	168	153	140	129	118

Applying the same techniques to the steps of all three step wedges, one can get 80 sets of experimental data, and each set contains g_1^L, g_2^L, and g_{Rgn}^L. If only one set of data is used, a^L can be computed as

$$a^L = \frac{255 g_{Rgn}^L}{g_1^L g_2^L} \tag{5.2-13}$$

To minimize the error, all 80 sets of data are used to compute a^L. The formula used is

$$a^L = \frac{\sum_n \frac{255 g_{Rgn}^L}{g_1^L g_2^L}}{n} \tag{5.2-14}$$

where n is the number of sets of data that are used for computing a^L. In this case, n is equal to 80. After computation, a^L is found to be 1.0898.

In order to determine the precision of Equation 5.2-12, the experimental data are collected from real-world objects as well as from the previously described step wedges. The real world objects included books, explosive simulants, Walkman cassette players, shampoo bottles, etc. The average gray level is computed for each object. An object, such as a book, is then overlapped with another object, such as a cassette player to form an object overlapped image region. The average gray level of this overlapped region is then measured. Using Equation 5.2-12 and the *true* gray levels of objects, a gray level is computed for this overlapped region. The error is computed using the following equation:

$$err = \frac{a^L \frac{g_1^L g_2^L}{255} - g_{Rgn}^L}{g_{Rgn}^L} \cdot 100\% \tag{5.2-15}$$

Table 5.2-3 gives some of the results obtained from this experiment. Column 1 is the gray level of Obj_1; column 2 is the gray level of Obj_2; column 3 is the measured gray level of the overlapped region *Rgn*; column 4 is the computed gray level of region *Rgn*; and column 5 is the errors computed using Equation 5.2-15.

The mathematical model of Equation 5.2-12 is quite precise in computing the gray levels for the overlapped region. For the 140 sets of data collected from the step wedges and the real-world objects, the errors are less than 4% for all the data sets. For some data sets, the errors are less than 1%.

Equation 5.2-12 can only be used to predict the gray level of an overlapped image region. Now, this equation is manipulated so that once the gray level of the overlapped region *Rgn* and the *true* gray level of the overlapping background object Obj_2 are known, the *true* gray level of the object of interest Obj_1 can be correctly computed. The equation for computing the *true* gray level of Obj_1 is as follows:

$$g_1^L = 255 \frac{g_{Rgn}^L}{a^L g_2^L} \tag{5.2-16}$$

One way to verify the precision of Equation 5.2-16 is to use a step wedge, for example, the clear step wedge as seen in Figure 5.2-2. Step 3 can be seen as step 2 overlaps with step 1. So knowing the gray level of step 2 and 3, the *true* gray level of step 1 can be computed using Equation 5.2-16. In Figure 5.2-2, the measured gray level of step 1 is 215; the computed *true* gray levels using step 2 is 209, step 3 is 212, step 4 is 211, step 5 is 213, step 6 is 211, step 7 is 210, and step 8 is 214. The verification in this case shows that the precision of Equation 5.2-16 is quite high. This is generally true for the other data sets that were collected.

Table 5.2-3 Computed gray levels of an overlapped region vs. the measured gray levels for some real-world objects in low-energy transmission modality

g_1^L	g_2^L	g_{Rgn}^L	$a^L \frac{g_1^L g_2^L}{255}$	Errors
215	215	192	197.6	2.9%
215	192	174	176.4	1.3%
215	174	157	159.9	1.8%
215	157	143	144.3	0.8%
215	143	129	131.4	1.8%
215	129	116	118.5	2.1%
215	116	106	106.6	0.6%
192	215	174	176.4	1.3%
192	192	157	157.6	0.4%
192	174	143	142.8	-0.2%
192	157	129	128.8	-0.1%
192	143	116	117.3	1.2%
192	129	106	105.9	-0.1%
174	215	157	159.8	1.8%
174	192	143	142.8	-0.2%
174	174	129	129.4	0.3%
174	157	116	116.8	0.7%
174	143	106	106.3	0.3%
157	215	143	144.3	0.9%
157	192	129	128.8	-0.1%
157	174	116	116.8	0.7%
157	157	106	105.3	-0.6%
143	215	129	131.4	1.9%
143	192	116	117.3	1.2%
143	174	106	106.3	0.3%
129	215	116	118.5	2.2%
129	192	106	105.9	-0.1%
116	215	106	106.6	0.6%

The derivation process of the overlap model for the high-energy transmission modality is exactly the same done for the low-energy transmission modality. The resulting equation is

$$g_{Rgn}^{H} = a^{H} \frac{g_1^{H} g_2^{H}}{255} \tag{5.2-17}$$

where g_1^H is the *true* gray level of Obj_1, the object of interest; g_2^H is the *true* gray level of Obj_2, the background overlapping object. g_{Rgn}^H is the gray level of the overlapped region *Rgn* that is formed by Obj_1 overlapping with Obj_2. a^H was found to be 1.0046 using experimental data that were collected and processed the same way as in low-energy transmission case. Table 5.2-4 gives some of the results obtained from the experiment in high-energy transmission modality. For the 140 sets of data collected from the step wedges and the real-world objects, the error of this formula is less than 1%. The error rate in high-energy transmission modality is smaller than in low-energy transmission modality because high-energy transmission images are less noisy than low-energy transmission images.

To compute the *true* gray level of Obj_1, the following equation can be used

$$g_1^{H} = \frac{255 g_{Rgn}^{H}}{a^{H} g_2^{H}}. \tag{5.2-18}$$

The precision of Equation 5.2-18 is also verified using a similar technique that was used in the low-energy transmission. Equation 5.2-18 is quite accurate in determining an object's *true* gray levels.

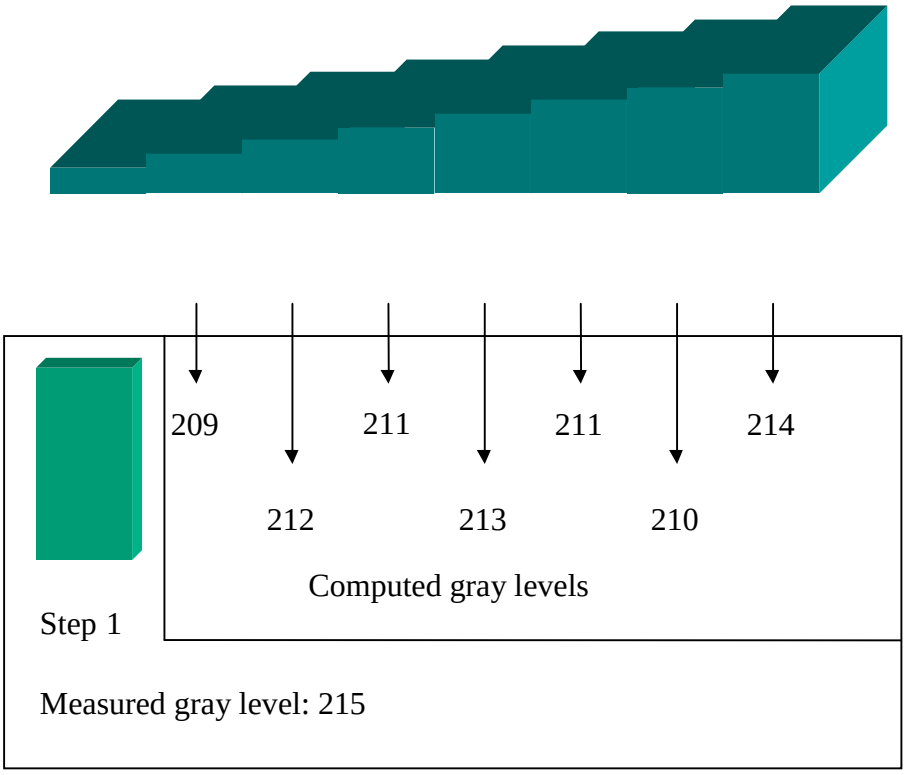

Figure 5.2-2 Results of the computed gray levels for step 1 of a clear plastics step wedge in low-energy transmission modality.

Table 5.2-4 Computed gray levels of an overlapped region vs. the measured gray levels for some real-world objects in high-energy transmission modality

g_1^H	g_2^H	g_{Rgn}^H	$a^H \frac{g_1^H g_2^H}{255}$	Errors
238	238	226	223.2	-1.3%
238	226	213	211.9	-0.5%
238	213	198	199.7	0.9%
238	198	186	185.7	-0.2%
238	186	175	174.4	-0.3%
238	175	165	164.1	-0.6%
238	165	155	154.7	-0.2%
226	238	213	211.9	-0.5%
226	226	198	201.2	1.6%
226	213	186	189.6	2.0%
226	198	175	176.3	0.7%
226	186	165	165.6	0.4%
226	175	155	155.8	0.5%
213	238	198	199.7	0.9%
213	226	186	189.6	2.0%
213	213	175	178.7	2.1%
213	198	165	166.2	0.7%
213	186	155	156.0	0.7%
198	238	186	185.7	-0.2%
198	226	175	176.3	0.7%
198	213	165	166.2	0.7%
198	198	155	154.5	-0.4%
186	238	175	174.4	-0.3%
186	226	165	165.6	0.4%
186	213	155	156.1	0.7%
175	238	165	164.1	-0.6%
175	226	155	155.8	0.5%
165	238	155	154.7	-0.2%

5.3 Forward-Scatter Overlap Models

The mathematical models for forward-scatter and backscatter overlap models are much more complicated than transmission overlap models. However, these formulas can still be derived in a similar manner as was employed to create transmission models. The undefined constants in the scatter overlap models can then be defined using experimental data. The accuracy of each formula is verified using more experimental data.

In forward-scatter modality, there are two different cases when two objects are overlapped. In case 1, Obj_1 is in front of Obj_2 as seen in Figure 5.1-1 (b). In case 2, Obj_1 is behind Obj_2 as seen in Figure 5.1-1 (c). Let us begin with the derivation of the mathematical formula for case 1 from the analysis model as seen in Figure 5.3-1. The following is a list of symbols used in the analysis model:

- Obj_1 – The object of interest.
- Obj_2 – The overlapping background object.
- I_0^L – The intensity of the incident x-ray beam.
- I_1^L – The transmission intensity after I_0^L traverses through Obj_1.
- I_1^F – The forward scatter intensity after I_0^L traverses through Obj_1.
- I_2^L – The transmission intensity after I_0^L traverses through Obj_2.
- I_2^F – The forward scatter intensity after I_0^L traverses through Obj_2.
- I_{2a}^L – The transmission intensity after I_1^L traverses through Obj_2.
- I_{2a}^F – The forward scatter intensity after I_1^L traverses through Obj_2.
- I_{2b}^F – The signal of I_1^F being transmitted through Obj_2. It is still a forward scatter signal.
- I_{2c}^F – The signal of I_1^F being scattered by Obj_2. It is a forward scatter signal.
- I_{Rgn}^F – The forward scatter intensity of the overlapped region.

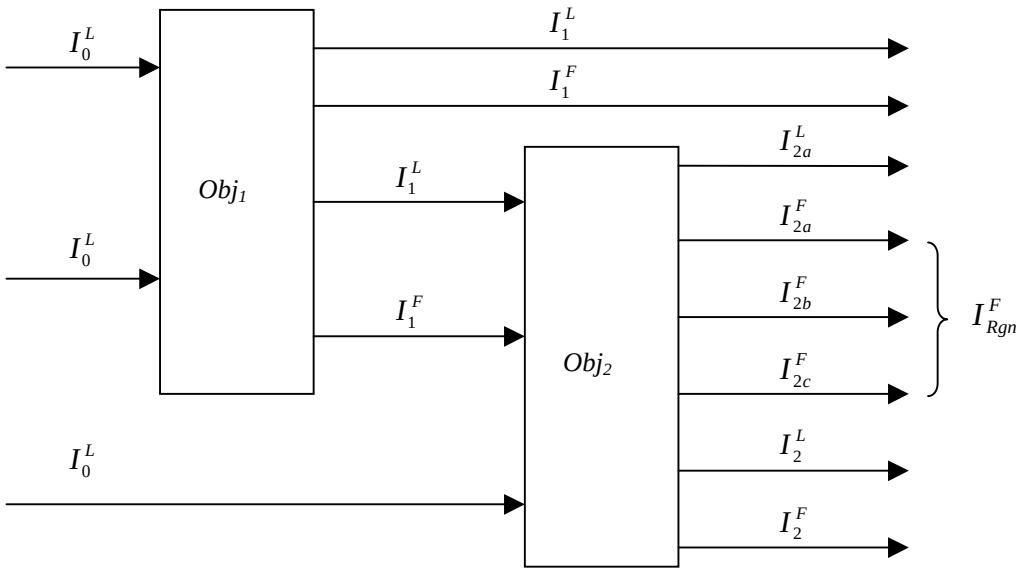

Figure 5.3-1 Analysis model for forward-scatter modality when two objects are overlapped. This figure shows the end view of the two objects Obj_1 and Obj_2, where Obj_1 is closer to the x-ray source than Obj_2.

This analysis model tries to resolve one issue: with knowledge of I_1^L and I_1^F from *Obj1*, and I_2^L and I_2^F from *Obj2*, how can the forward-scatter x-ray intensity I_{Rgn}^F for the overlapped region *Rgn* be computed when *Obj1* is overlapped with *Obj2*, and *Obj1* is closer to the x-ray source. The assumption is that regardless of the intensity and types of incident x-ray beams, the portions of the x-ray intensity that are being transmitted and forward scattered by *Obj2* remain constant. The portion being transmitted can be computed as I_2^L / I_0^L. The portion being forward scattered can be computed as I_2^F / I_0^L.

When a beam of x-ray I_0^L first traverses through *Obj1*, then traverses through *Obj2*, the following process happens. The incident x-ray beam I_0^L interacts with *Obj1*, yields a transmission signal I_1^L, and a forward scatter signal I_1^F in the forward direction. The transmission signal I_1^L interacts with *Obj2* and yields a transmission signal I_{2a}^L and a forward scatter signal I_{2a}^F. The forward scatter signal I_1^F interacts with *Obj2*, the signal being transmitted when traversing through *Obj2* is I_{2b}^F, which is still a forward-scatter signal; and the signal being forward scattered by *Obj2* is I_{2c}^F.

I_{2a}^F can be computed as $I_1^L\left(\frac{I_2^F}{I_0^L}\right)$, where I_1^L is the incident x-ray beam to *Obj2*, and $\frac{I_2^F}{I_0^L}$ is the fraction of incident x-ray that is forward scattered.

I_{2b}^F can be computed as $I_1^F\left(\frac{I_2^L}{I_0^L}\right)$, where I_1^F is the incident x-ray forward scatter energy to *Obj2*, and $\frac{I_2^L}{I_0^L}$ is the fraction of the scattered signal that is transmitted by *Obj2*.

I_{2c}^F can be computed as $I_1^F\left(\frac{I_2^F}{I_0^L}\right)$, where $\frac{I_2^F}{I_0^L}$ is the fraction of the scattered signal that is scattered by *Obj2*.

Thus, the combination of the signal $\left(I_{2b}^F + I_{2c}^F\right)$ can be computed as $\alpha_1^F \frac{I_1^F}{I_0^F}\left(I_2^L + \alpha_2^F I_2^F\right)$, where α_1^F and α_2^F are two constants used to calibrate the results. The calibration is needed because the x-ray source is not an ideal parallel source, and the geometry of the forward-scatter detectors needs to be considered as well.

$\alpha_1^F \frac{I_1^F}{I_0^F}\left(I_2^L + \alpha_2^F I_2^F\right)^2$ is used to account for the non-linear part of the signal $\left(I_{2b}^F + I_{2c}^F\right)$ that is ignored by $\alpha_1^F \frac{I_1^F}{I_0^F}\left(I_2^L + \alpha_2^F I_2^F\right)$.

In summary, I_{Rgn}^F, the forward scatter intensity of the overlapped region *Rgn* is the summation of I_{2a}^F, I_{2b}^F, and I_{2c}^F. It can be computed as:

$$\begin{aligned} I_{Rgn}^F &= I_{2a}^F + I_{2b}^F + I_{2c}^F \\ &= I_1^L\left(\frac{I_2^F}{I_0^L}\right) + \alpha_1^F \frac{I_1^F}{I_0^L}\left(I_2^L + \alpha_2^F I_2^F\right) + \alpha_1^F \frac{I_1^F}{I_0^L}\left(I_2^L + \alpha_2^F I_2^F\right)^2 \\ &= I_1^L \frac{I_2^F}{I_0^L} + \beta_1^F \frac{I_1^F}{I_0^L} I_2^L + \beta_2^F \frac{I_1^F}{I_0^L} I_2^{L^2} + \beta_3^F \frac{I_1^F}{I_0^L} I_2^F + \beta_4^F \frac{I_1^F}{I_0^L} I_2^{F^2} + \beta_5^F \frac{I_1^F}{I_0^L} I_2^F I_2^L \end{aligned} \quad (5.3\text{-}1)$$

The last line of this equation is the expansion of the next to last line. Since the terms of $\frac{I_1^F}{I_0^L} I_2^{L^2}$ and $\frac{I_1^F}{I_0^L} I_2^{F^2}$ do not contribute much to the overall computation of I_{Rgn}^F, they are ignored.

After simplification of Equation 5.3-20, the equation becomes:

$$I_{Rgn}^F = \alpha_1^F I_1^L I_2^F + \alpha_2^F I_1^F I_2^L + \alpha_3^F I_1^F I_2^F \quad (5.3\text{-}2)$$

When converted in the form of gray levels, Equation 5.3-2 becomes:

$$g_{Rgn}^{F} = \alpha_1^F g_1^L g_2^F + \alpha_2^F g_1^F g_2^L + \alpha_3^F g_1^F g_2^F \tag{5.3-3}$$

where g_1^L is the *true* transmission gray level of *Obj1*; g_1^F is the *true* forward-scatter gray level of *Obj1*. g_2^L is the *true* transmission gray level of *Obj2*. g_2^F is the *true* forward scatter gray level of *Obj2*. g_{Rgn}^F is the computed gray level of the overlapped region. Note: the conversion factors c^F and c^L have been absorbed into α_1^F, α_2^F, and α_3^F.

The values of α_1^F, α_2^F, and α_3^F are computed using the experimental data collected from the three step wedges. The method for data collection from those three step wedges is almost exactly the same as the method used in the transmission modality. The difference is that for each step of a step wedge, the average gray level in low-energy transmission modality is measured; the average gray level in the forward-scatter modality is also measured. So each set of data is comprised by six gray levels: g_1^L, g_1^F, g_2^L, g_2^F, g_{Rgn}^L, and g_{Rgn}^F. 80 sets of those data are collected from three step wedges. Using least-square-error fitting method, the values of those constants are found to be $\alpha_1^F = 0.0018$, $\alpha_2^F = 0.0032$, and $\alpha_3^F = 0.0016$.

Figure 5.3-2 shows the comparison between the measured g_{Rgn}^F and the computed g_{Rgn}^F for some steps of a white plastic step wedge. The errors in this case are very small. Equation 5.3-4 works well with materials such as white plastics. What is particularly interesting is that this equation successfully predicted that the gray level decrease when the thickness of the object increases beyond a certain threshold. This prediction can be observed in Figure 5.3-2. Note: the larger the step number is, the thicker the overlapped region.

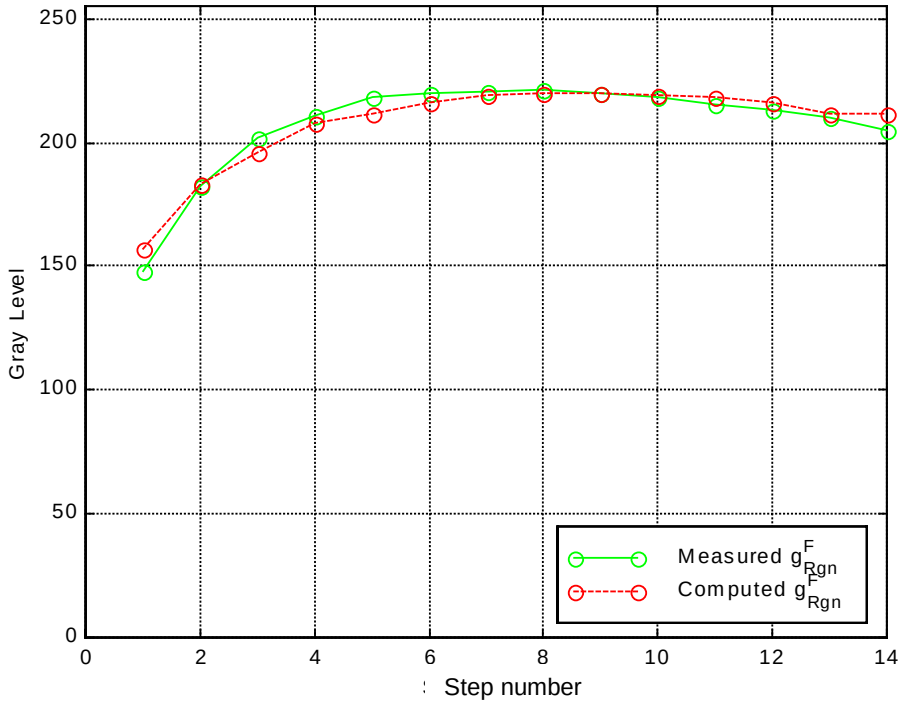

Figure 5.3-2 Comparison between the measured gray level of the overlapped region *Rgn* and the computed gray level of *Rgn* for some steps of a white plastic step wedge in the forward scatter modality.

However, Equation 5.3-3 does not work well with other materials. For some real-world objects that were tested, the computation error is greater than 5%. Some of the results are shown later in this section. There are many sources that might contribute to this error. For example, the x-ray source is not an ideal parallel source. The detector geometry affects the collection of forward-scatter x-ray signals. It was assumed that the fraction of the incident x-ray being transmitted or forward scattered is constant. This may only be true in the first order approximation, but not in higher orders. The noise of the forward scatter images is significantly larger than the transmission images. This may affect the precise computation of image gray levels.

The scattered radiation has a lower frequency than the transmission wavelength and hence has less penetration power. Thus the fraction of a forward scattered signal that is being forward scattered should not be the same as the fraction of a transmitted signal that is being forward scattered. Unfortunately, there is no way that the first fraction can be directly measured or derived in the current experimental condition. One less perfect solution is to assume that those two fractions are the same. This assumption may have contributed significant amount of computation error to the overlap model.

Due to the limitation of our equipment and funding, it is difficult to quantify the amount of error that each of the above sources is likely to contribute. This forward scatter overlapping model can be further improved if one has the ability to determine the major source of error and to fix the model in that aspect. This mathematical model can also be improved if for different material or object thickness, different equations are used. However, refining this model is beyond the scope of this research. It can be done if there is enough funding to support another 3 or 4 year of research.

Using Equation 5.3-4, the background overlap effect can be eliminated – though the computation may not be that accurate. Assume Obj_1 is the object of interest, and Obj_2 is the background overlap object. Assume that the *true* transmission gray level of Obj_2 g_2^L is known; the *true* forward-scatter gray level of Obj_2 g_2^F is known; the forward-scatter

gray level of the overlapped region *Rgn* g_{Rgn}^{F} is also known. The *true* transmission gray level of *Obj1* g_1^L can be computed using Equation 5.2-16. The *true* forward-scatter gray level of *Obj1* can be computed as:

$$g_1^F = \frac{g_{Rgn}^F - \alpha_1^F g_1^L g_2^F}{\alpha_2^F g_2^L + \alpha_3^F g_2^F} \tag{5.3-4}$$

The forward-scatter overlap model for case 2 of the two-object-overlap problem can be derived in a similar manner. The mathematical model that results is:

$$g_{Rgn}^F = \alpha_1^F g_2^L g_1^F + \alpha_2^F g_2^F g_1^L + \alpha_3^F g_2^F g_1^F \tag{5.3-5}$$

where α_1^F *=0.0018*, α_2^F *=0.0032*, and α_3^F *=0.0016*. The accuracy of this equation is the same as the accuracy of Equation 5.3-4. By manipulating this equation, the *true* forward-scatter gray level of *Obj1* can be computed:

$$g_1^F = \frac{g_{Rgn}^F - \alpha_2^F g_2^F g_1^L}{\alpha_1^F g_2^L + \alpha_3^F g_2^F} \tag{5.3-6}$$

Apparently, since Equation 5.3-3 and 5.3-5 are not very accurate in modeling forward-scatter overlap, the *true* gray levels computed using Equation 5.3-4 and 5.3-6 are not very accurate either.

Table 5.3-1 shows the computed *true* gray levels vs. the measured *true* gray levels for some objects of interest using Equations 5.3-4 and 5.3-6. Column 1 is the gray level of the overlapped region formed by an object of interest and another background object. Column 2 is the measured *true* gray level of that object of interest. Column 3 is the computed *true* gray level of the objects of interest.

Table 5.3-1 Computed *true* gray levels of an object of interest vs. the measured *true* gray levels for some real-world objects in forward scatter modality

g_{Rgn}^{F}	g_{1}^{F}	$\tilde{g}_{1}^{F}$	Errors
106	98	98	0.0%
113	128	124	-3.1%
110	149	131	-12.1%
103	157	146	-7.0%
98	160	167	4.4%
92	162	188	16.0%
92	158	188	19.0%
106	87	85	-2.3%
113	97	90	-7.2%
110	98	86	-12.2%
103	96	91	-5.2%
98	94	94	0.0%
92	91	107	17.6%
92	88	107	21.6%
115	104	110	5.8%
124	139	143	2.9%
112	163	126	-22.7%
118	112	103	0.6%
110	182	196	7.7%
91	186	180	-3.2%
91	185	180	-2.7%

Column 4 is the error of computation calculated using the following equation:

$$err=\frac{\tilde{g}_1^F - g_1^F}{g_1^F}\cdot 100\% \tag{5.3-7}$$

where $\tilde{g}_1^F$ is the measured *true* gray level of the object of interest.

By examining Column 4 in Table 5.3-1, one may find that although most computation errors are within 10%, but some of the computation errors are over 20%. The error is too large for accurate *true* gray level computations. However, when the data in Column 1 and the data in Column 2 are carefully compared, one can easily see that the measured gray level at an overlapped region is significantly different from the measured *true* gray level of the object of interest. The gray level at Column 1 cannot be used to represent the *true* gray level of an object of interest. The computed *true* gray level shown at Column 3 is much closer to the measured *true* gray level shown at Column 2. Although the errors of this model are still too large, the development of such a model represents a step forward. Further improvement to this model will not only benefit the *true* gray level computation, it will also directly contribute to the material characterization using *R-L* plane method.

5.4 Backscatter Overlap Models

Figure 5.4-1 shows the analysis model for case 1 of the two-object-overlap problem, which is described in Figure 5.1-1. Obj_1 is closer to the x-ray source than Obj_2. The following is a list of symbols used in the analysis model:

- I_1^B – The intensity of the backscattered signal after I_0^L interacts with Obj_1.
- I_2^B – The intensity of the backscattered signal after I_0^L interacts with Obj_2.
- I_{2a}^B – The intensity of the backscattered signal after I_1^L and I_1^F interacts with Obj_2.

- I_{1a}^{B} – The intensity of the backscattered signal after I_{2a}^{B} interacts with *Obj₁*.
- I_{Rgn}^{B} – The intensity of the backscattered signal of the overlapped region.

The assumption in this model is that regardless of the intensity and type of incident x-ray beam, the fractions of signal being transmitted and forward scattered by *Obj₁* remain constant; the fraction of signal being backscattered by *Obj₂* remain constant as well. The faction of signal that is transmitted by *Obj₁* can be computed as I_1^L / I_0^L. The faction of signal that is forward scattered by *Obj₁* can be computed as I_1^F / I_0^L. The fraction of signal that is backscattered by *Obj₂* can be computed as I_2^B / I_0^L.

The backscatter process of two objects in an overlapping situation can be explained as follows. When the incident x-ray beam I_0^L interacts with *Obj₁*, the signal being backscattered by *Obj₁* is I_1^B; the signal being transmitted is I_1^L; and the signal being forward scattered is I_1^F. The incident x-ray to *Obj₂* is $\left(I_1^L + I_1^F\right)$. The signal being backscattered by *Obj₂* is I_{2a}^B. I_{2a}^B becomes the incident x-ray to *Obj₁*. The signal being transmitted and forward scattered is I_{1a}^B. So the total backscattered signal I_{Rgn}^B is equal to $\left(I_1^B + I_{1a}^B\right)$.

Signal I_{1a}^B can be computed as the summation of $I_{2a}^B\left(\frac{I_1^L}{I_0^L}\right)$ and $I_{2a}^B\left(\frac{I_1^F}{I_0^L}\right)$, where $\frac{I_1^L}{I_0^L}$ is the fraction of I_{2a}^B that is being transmitted by *Obj₁*, and $\frac{I_1^F}{I_0^L}$ is the fraction of I_{2a}^B that is being forward scattered by *Obj₁*.

Signal I_{2a}^B can be computed as $\left(I_1^F + I_1^L\right)\left(\frac{I_2^B}{I_0^L}\right)$, where $\left(I_1^F + I_1^L\right)$ is the incident signal to *Obj₂*, and $\frac{I_2^B}{I_0^L}$ is the fraction of signal being backscattered by *Obj₂*.

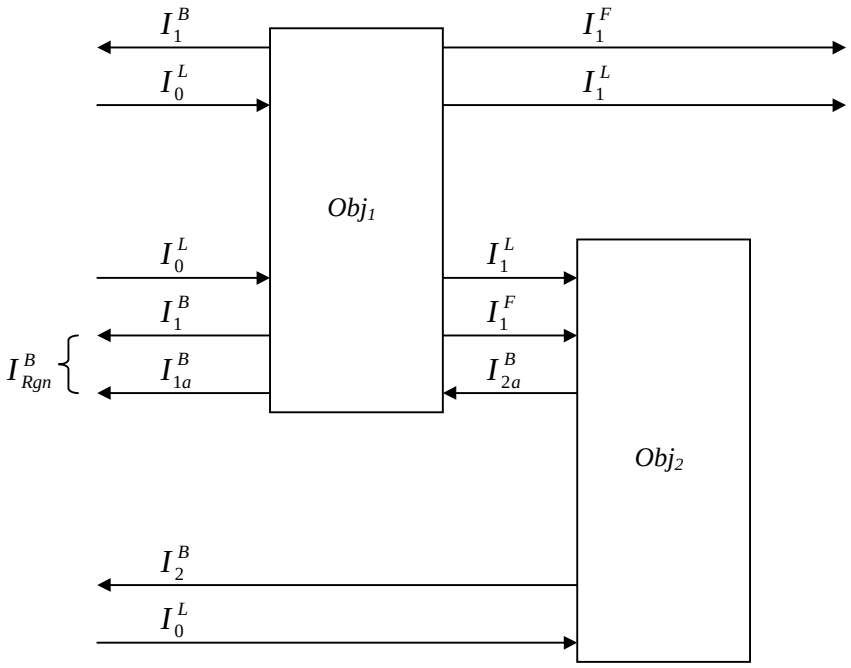

Figure 5.4-1 Analysis model for backscatter modality when two objects are overlapped. This figure shows the end view of Obj_1 and Obj_2, where Obj_1 is the object of interest, and is closer to the x-ray source than Obj_2.

Signal I_{Rgn}^{B}, the backscatter signal of the overlapped region *Rgn* can be computed as the summation of $\left(I_1^B + I_{1a}^B\right)$. Now the mathematical model can be written as follows:

$$\begin{aligned} I_{Rgn}^{B} &= I_1^B + I_{1a}^B \\ &= I_1^B + \frac{I_1^L}{I_0^L} I_{2a}^B + \frac{I_1^F}{I_0^L} I_{2a}^B \\ &= I_1^B + \alpha_1^B \frac{I_1^L}{I_0^L}\frac{I_2^B}{I_0^L}\left(I_1^L + I_1^F\right) + \alpha_2^B \frac{I_1^F}{I_0^L}\frac{I_2^B}{I_0^L}\left(I_1^L + I_1^F\right) \\ &= I_1^B + \beta_1^B \left(I_1^L\right)^2 I_2^B + \beta_2^B I_1^L I_2^B I_1^F + \beta_3^B \left(I_1^F\right)^2 I_2^B \end{aligned} \tag{5.4-1}$$

Due to system noise and some other factors, the results computed for the signal backscattered by *Obj₂* need some calibration. α_1^B and α_2^B are the two constants used to calibrate the results. Row four of this equation is the expansion of row three.

Equation 5.4-1 is then converted in the form of gray levels. The conversion factors c^L, c^F, and c^B are absorbed into α_1^B, α_2^B, and α_3^B. The equation can then be written as:

$$g_{Rgn}^{B} = g_1^B + \alpha_1^B \left(g_1^L\right)^2 g_2^B + \alpha_2^B g_1^L g_2^B g_1^F + \alpha_3^B \left(g_1^F\right)^2 g_2^B \tag{5.4-2}$$

Using a manner similar to both transmission and forward scatter model development, 80 sets of data were collected from the three step wedges. Each set of data contains 9 gray levels. For *Obj₁*, the gray levels include the *true* transmission gray level g_1^L; the *true* forward-scatter gray level g_1^F; and the *true* backscatter gray level g_1^B. For *Obj₂*, the gray levels include the *true* transmission gray level g_2^L; the *true* forward-scatter gray level g_2^F; and the *true* backscatter gray level g_2^B. For the overlapped region *Rgn*, the gray levels include the *true* transmission gray level g_{Rgn}^L; the *true* forward-scatter gray level g_{Rgn}^F; and the *true* backscatter gray level g_{Rgn}^B. Using this data the constants α_1^B, α_2^B,

and α_3^B can be determined using a least-square method. They are found to be α_1^B=0.4761, α_2^B=-0.1639, and α_3^B=0.0138.

Figure 5.4-2 shows the comparison between the measured g_{Rgn}^B and the computed g_{Rgn}^B for some steps of a white plastic step wedge. The errors in this case are extremely small; but this is not generally true for many other objects that were tested. In some cases, Equation 5.4-2 has computation errors that are greater than 10%. Some of the computation results are shown later in this section. The sources of error are basic the same as in the forward-scatter modality. In addition, the computation of *true* gray level in backscatter modality relies on the knowledge of *true* gray level in forward scatter modality. Since no accurate *true* gray level in forward scatter modality can be calculated, the *true* gray level in backscatter modality cannot be accurate calculated. The solutions to improve this model are also the same as in the forward-scatter modality.

Assume Obj_1 is the object of interest, and Obj_2 is its overlapping background object. After manipulating Equation 5.4-2, the following equation is used for compute the *true* backscatter gray level of Obj_1 for case 1 of the two-object-overlapping problem:

$$g_1^B = g_{Rgn}^B - \alpha_1^B \left(g_1^{L^2} + g_2^B \right) - \alpha_2^B g_1^L g_2^B g_1^F - \alpha_3^B g_1^{F^2} g_2^B \tag{5.4-3}$$

Assume now Obj_1 is further to the x-ray source than Obj_2. This is case 2 of the two-object-overlapping problem, as seen in Figure 5.1-1 (c). Using similar manner, the equation for computing the *true* backscatter gray level of Obj_1 can be derived. The equation is as follows:

$$g_1^B = \frac{g_{Rgn}^B - g_2^B}{\alpha_1^B g_2^{L^2} + \alpha_2^B g_2^L g_2^F + \alpha_3^B g_2^{F^2}} \tag{5.4-4}$$

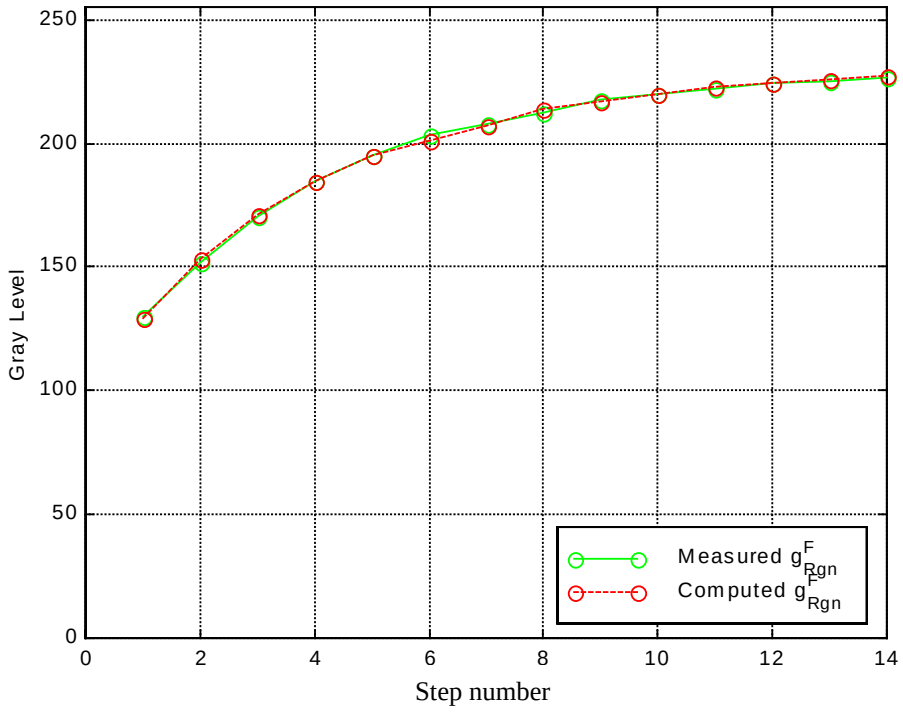

Figure 5.4-2 Comparison between the measured gray level of the overlapped region *Rgn* and the computed gray level of *Rgn* for some steps of a white plastic step wedge in the forward-scatter modality.

Since the mathematical overlap models for backscatter modality are not very accurate, the *true* backscatter gray levels that are computed using Equation 5.4-3 and 5.4-4 are not very accurate either.

Table 5.4-1 shows some computation results using the backscatter overlapping models. Column 1 is the measured gray level of the overlapped region that is formed by an object of interest and its background object. Column 2 is the measured *true* gray level of an object of interest. Column 3 is the computed *true* gray level of an object of interest. Column 4 is the computation error that is calculated using the following equation:

$$err = \frac{\tilde{g}_1^B - g_1^B}{g_1^B} \cdot 100\% \qquad (5.4\text{-}5)$$

where $\tilde{g}_1^B$ is the measured *true* gray level of the object of interest. Most of the computation errors are over 10%. However, most of the errors may have been caused by not knowing the accurate *true* gray levels in forward scatter modality. It is author's belief that if the accurate *true* gray level in forward scatter modality can be computed, the error of the backscatter overlap model should be less than 10%.

In summary, from Section 5.2 to Section 5.4, the discussion has focused on developing models for the two-object-overlap problems. There is a model for each sensing modality. Each model is first derived using mathematical formulas with undefined constants. The values of those constants are then computed using experimental data collected from the three step wedges. The accuracy of each model is then verified using real-world objects. The transmission overlap models work quite precise. The forward scatter and backscatter overlap models need further refinement, since the scatter models are just a 1st order approximation. However, to refine those models is beyond the scope of this study; it can be done, but would take some considerable effort.

Table 5.4-1 Computed *true* gray levels of an object of interest vs. the measured *true* gray levels for some real-world objects in backscatter modality

g_{Rgn}^{B}	g_{1}^{B}	$\tilde{g}_{1}^{B}$	Errors
105	92	109	18.5%
135	120	142	18.3%
152	142	161	13.4%
166	158	176	11.4%
177	168	184	9.5%
188	176	198	12.5%
188	182	198	8.8%
198	188	208	10.6%
87	90	92	2.2%
97	114	105	-7.9%
95	131	103	-21.4%
99	140	109	-22.1%
99	126	105	-16.7%

5.5 The Algorithm for Determining the Object's *True* Gray Levels

In this section, the algorithm for computing the *true* gray levels of an object of interest is discussed in detail. First, a brief introduction is given here as the background to the algorithm development.

As discussed earlier in Section 4.4, an object of interest *Obj* is more likely to be segmented into several different regions in Img_{Rgn}^{Lbl}, for example *Rgn*, *Rgn'*, etc.; but *Obj* is more likely to be segmented into one object in Img_{Obj}^{Lbl}. Img_{Rgn}^{Lbl} and Img_{Obj}^{Lbl} are perfectly spatially registered. If a region in Img_{Rgn}^{Lbl} have 70% of its pixels belonging to *Obj*, this region should be part of *Obj*. Using this method, *Rgn* and other regions that belong to *Obj* are identified and grouped. In other words, segmented labeled components in Img_{Rgn}^{Lbl} can be referred as regions, and each component is denoted by *Rgn*. Segmented labeled components in Img_{Obj}^{Lbl} can be referred as objects, and each component is denoted by *Obj*. For each region *Rgn*, an object *Obj* can always be found where $Rgn \in Obj$.

It is impossible to correctly resolve the overlap problem since one can never know from a 2-D image whether overlap occurs or not. The principle of this algorithm is to apply some exterior criteria to the image in order to determine the *true* gray level of an object of interest. The algorithm development is concentrated on the *true* gray level computation in the transmission modalities due to three important considerations. First, the accuracy of the forward scatter and backscatter modalities still need some improvement, so it is impossible in the current situation to create an algorithm that can accurately calculate *true* gray levels in either of the scatter modality using those models. Second and most importantly, if this algorithm works in the transmission modalities, just by using more accurate scatter overlap models, the *true* gray levels can be easily computed in scatter modalities. Third, although the scatter data is missing, the dual-energy transmission data computed using this algorithm at least allows one to distinguish organic materials from inorganic materials.

Knowing only the models for eliminating the background effects will not allow one to correctly compute the *true* gray levels of an object of interest. This is because the luggage inspection problem overlapping situations are typically quite complex. One such example is given in Figure 5.5-1. In Figure 5.5-1 (a), two regions are observed in a 2-D x-ray image. Those two regions may be formed by two objects that are placed side-by-side as seen in Figure 5.5-1 (b) or by two objects that are overlapped as seen in Figure 5.5-1 (c). Being able to correctly interpret such kinds of scenarios is crucial towards the computation of *true* gray levels of an object of interest. Another example is that in a bag image, an object of interest is often surrounded by many neighboring regions. Being able to determine the correct neighboring region that represents the background object is another problem that needs to be correctly resolved. The methods that are used to revolve those issues are discussed in this section. These methods are implemented in the procedure *true_gl()*.

The principle of computing *true* gray levels is to find a special neighboring region to an object of interest, and use this neighboring region's gray level information to compute the *true* gray level of the object of interest. This special region is a region that is most likely to be part of the object that overlaps with the object of interest.

As discussed in Section 4.3, objects in a bag can generally be classified into two categories: *textile* objects and *solid* objects. *Textile* objects are objects without constant shape. *Solid* objects are objects with constant shape. Explosives including plastic explosives are considered as *solid* objects. Consequently, the objects of interest for this image-processing system are *solid* objects. Now using these concepts, the typical object layout in a bag is analyzed. Problems that might prevent the computation of the *true* gray levels of an object are identified. Solutions to those problems are presented.

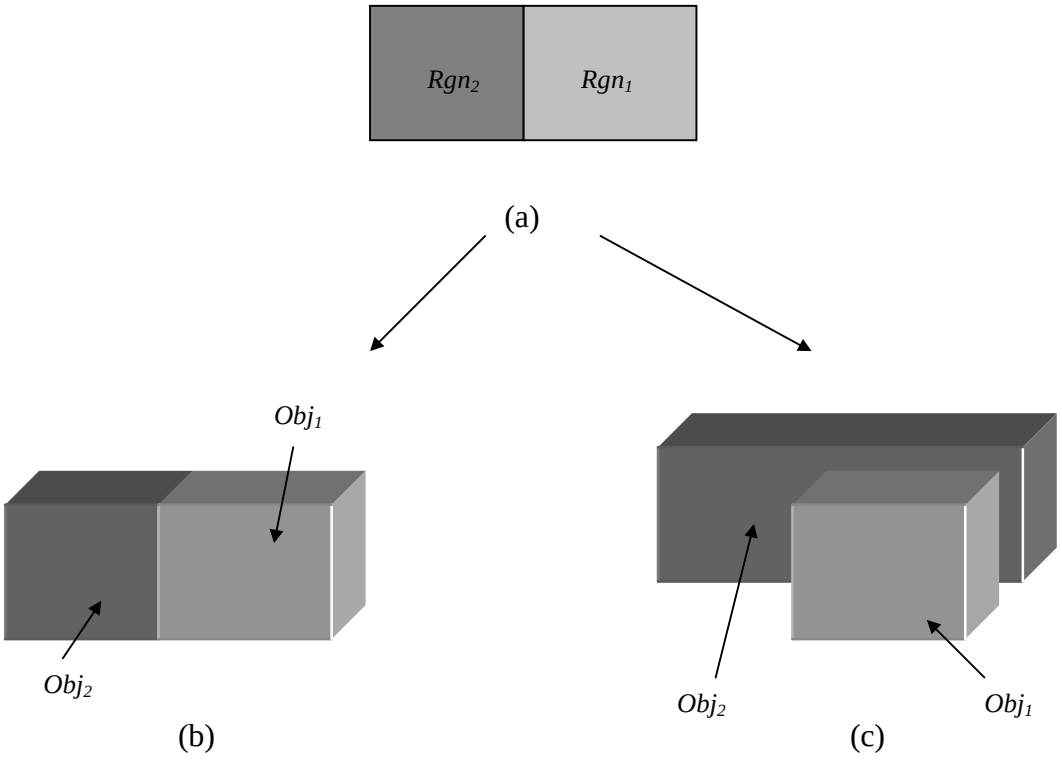

Figure 5.5-1 Interpretation of an image scenario. The image scenario shows in a) in a one-view image may be interpreted as two objects are placed side by side as seen in b), or Obj_2 is the background object of Obj_1 as seen in c).

The typical object layout in luggage is shown in Figure 5.5-2. The left drawing in this figure is the side view of a bag, and the right drawings represent end views of the bag. The side view is the view from which the AS&E system would collect images. The end view is the view that one may observe from the traveling direction of the bag; the end view is used to illustrate the overlapping situations. In a bag, the bag covers or sides always appear. So every object of interest will be at least overlap with those bag covers. In most cases, people stuff their luggage with towels, socks, and clothes, all of which are *textile* objects. So an object of interest will also overlap with these *textile* objects as well. However, when *solid* objects overlap with *textile* objects, in many cases, the *textile* objects will not significantly contribute to the overlapped regions. They may cause 2 or 3 gray level variations. Consider that the noise of the system may cause up to 7 gray level variations, those effects caused by *textile* objects can generally be ignored. In case 3, an object of interest is overlapped with another *solid* object. The development of *true_gl()* is based on handling the object layouts shown in this.

The inputs to routine *true_gl()* are four perfectly registered images: Img_{Smth}^{L}, Img_{Smth}^{H}, Img_{Rgn}^{Lbl}, and Img_{Obj}^{Lbl}. For convenience, the labeled components in Img_{Rgn}^{Lbl} are called regions and the labeled components in Img_{Obj}^{Lbl} are called objects.

Since explosives are considered as *solid* objects, and *solid* objects are usually segmented into regions larger than 400 pixels in Img_{Rgn}^{Lbl}, only regions with size larger than 400 pixels are considered by *true_gl()*.

Symbol Obj_1 always represents the object of interest. In a low-energy transmission image, a region of interest *Rgn*, where $Rgn \in Obj_1$, may represent a situation where an object of interest Obj_1 only overlaps with the bag covers and other *textile* objects, as seen in case 2 of Figure 5.5-2. In this case, g_1^L, the *true* gray level of Obj_1 can be determined if the overlap effects caused by the bag covers and the *textile* objects are removed.

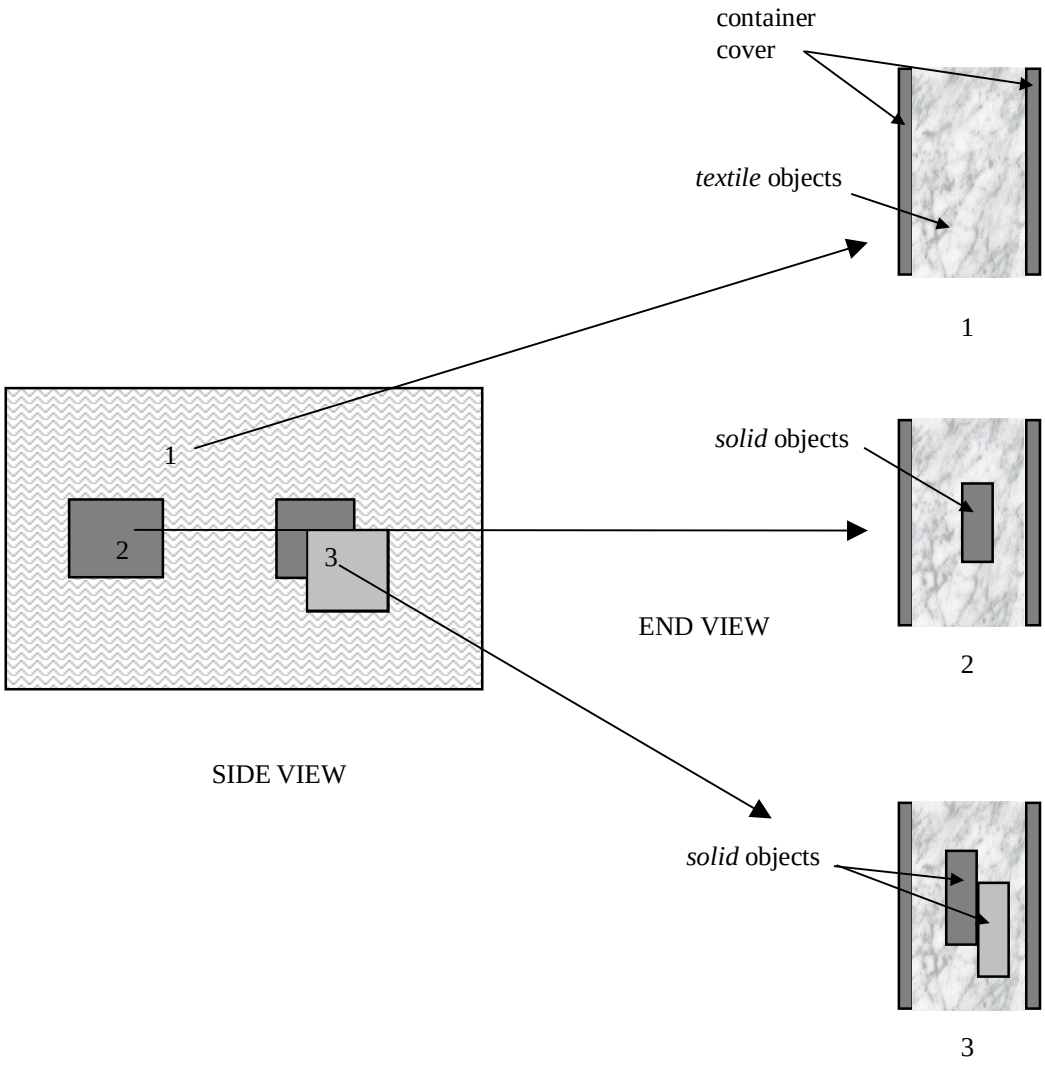

Figure 5.5-2 Illustration of commonly seen object layout in a bag. The left graph is a side view image, and the right three graphs are three typical object layouts. Layout type one is when only some *textile* objects appear at a region. Layout type two is that a *solid* object is overlapped with some *textile* objects. Layout type three is that a *solid* object is overlapped with some other *solid* objects, and those *solid* objects are overlapped with some *textile* objects.

One valid assumption is that the overlapping effects caused by the bag covers are the same everywhere in a bag. If the region where only bag covers are found, the gray level of this region can then be used to remove the effects caused by the bag covers. Denote this region as Rgn_{Cover}, and the gray level of this region as g^L_{Cover}. Rgn_{Cover} should be the brightest region in a low-energy transmission image. Knowing the average gray level of region *Rgn*, g^L_{Rgn}, and the *true* gray level of Obj_1, g^L_{Cover}, the *true* gray level of Obj_1, g^L_1, can then be computed using Equation 5.2-16. This computation basically ignores the effects caused by the *textile* objects that are inserted between the *solid* objects and the bag covers.

However, besides overlapping with the bag covers and other *textile* objects, the region of interest *Rgn* may also be formed by Obj_1 overlapping with another *solid* object Obj_2 besides those bag covers and some *textile* objects as seen in case 3 of Figure 5.5-2. To compute the *true* gray level of Obj_1, g^L_{Rgn}, and the gray level of a neighboring region Rgn_2 needs to know. Region Rgn_2 is the region that belongs to Obj_2. Part of Obj_2 overlaps with the object of interest Obj_1 that forms *Rgn*; part of Obj_2 only overlaps with the bag covers and some *textile* objects that forms Rgn_2. Region Rgn_2 should be one of the neighboring regions of *Rgn*.

It is very difficult to determine which neighboring region of *Rgn* is Rgn_2. Some of the neighboring regions are eliminated from the candidate list because they cannot be Rgn_2. Region Rgn_2 should always be brighter than *Rgn* because Obj_2, where $Rgn_2 \in Obj_2$, forms the region of *Rgn*. In the transmission modality, an overlapped region should always be darker than the object that forms this region. So if a neighboring region is darker than region *Rgn*, it should be eliminated from the candidate list. Region Rgn_2 should also have some percentage of common boundaries with *Rgn*. If the common boundary between a candidate region and *Rgn* is less than 5% of the perimeter of *Rgn*, it is also unlikely that this region is a candidate for Rgn_2. Hence it should be eliminated from the candidate list. In addition, the candidate *true* gray level computed using g^L_{Cover} is also added to the list. After region elimination using these conditions, the number of

candidate regions should be around 2 to 4. A list of candidate *true* gray levels of *Rgn* is computed using g_{Rgn}^{L} and the gray levels of those candidate neighboring regions.

As we know that $Rgn \in Obj_1$. The next goal is to find the *true* gray level of Obj_1. All regions, for example *Rgn*, *Rgn'*, etc., that belong to Obj_1 can be found using the method mentioned at the beginning of this section. After all such regions have been identified, a list of candidate *true* gray levels for Obj_1 is created. It includes all the candidate *true* gray levels of all the regions that belong to Obj_1. The *true* gray level Obj_1 is the candidate gray level that occurs with the highest frequency in the list.

In high-energy transmission modality, the procedure for determining the *true* gray level of Obj_1, g_1^H, is exactly the same as in low-energy transmission modality. Note: the brightest region in the low-energy transmission image should also be the brightest region in the high-energy transmission image.

Although this algorithm was not implemented in the forward scatter and backscatter modalities, the procedure for determining the *true* gray levels of Obj_1, g_1^F and g_1^B, are no different than in either the low- or high-energy transmission modality. Once those scatter models are refined, this algorithm can easily be modified to handle the computation in all four sensing modalities.

The complete procedure in transmission modalities is described as follows:

Procedure *true_gl()*

1. Compute the size and boundary length of each region in Img_{Rgn}^{Lbl}.
2. For each region in Img_{Rgn}^{Lbl}, compute the average gray level of its corresponding region in Img_{Smth}^{L}.
3. Find the brightest region of Img_{Smth}^{L} that is at least 400 pixel in size.

4. For a region *Rgn* in Img_{Rgn}^{Lbl}, use the brightest region together with all selected neighbors of *Rgn* to compute a list of possible *true* gray levels for *Rgn* in low-energy transmission modality. A selected neighbor should be brighter than *Rgn*; and the common boundary between the neighbor and *Rgn* should be greater than 5% of the perimeter of *Rgn*.
5. Repeat step 4 for all regions in Img_{Rgn}^{Lbl}.
6. For an object Obj_1 in Img_{Rgn}^{Obj} with at least 400 pixels in size, determine all the regions in Img_{Rgn}^{Lbl} that belong to Obj_1.
7. The candidate *true* gray levels for an object Obj_1 in Img_{Rgn}^{Obj} include all the candidate *true* gray levels of regions that belong to Obj_1.
8. The *true* gray level for an object Obj_1 in Img_{Rgn}^{Obj} is the one that occurs the most frequent in the candidate list.
9. Repeat step 6 to 8 for all objects in Img_{Rgn}^{Obj}.
10. Repeat step 1 to 9 to compute the *true* gray levels for all regions in Img_{Smth}^{H}.

Procedure *true_gl()* reports a list of *solid* objects along with their *true* gray levels in low- and high-energy transmission modalities. A typical report format is as follows:

Object Number	*True* gray level in Img_{Smth}^{L}	*True* gray level in Img_{Smth}^{H}
2	50	70
3	20	50
...	...	...

Note that the object number refers to the label used in Img_{Rgn}^{Obj}.

5.6 Chapter Summary

In this chapter, the development of the module for determining an object's *true* gray levels is discussed. The development of this module was done in two stages. At the first stage, overlap models are developed for each of the different sensing modalities. The high-energy and low-energy overlap models are quite precise in determining an object's *true* gray levels. Although the forward-scatter and backscatter overlap models have not achieved the needed computation precision, they have significantly improved one's ability to compute the *true* gray levels in those two sensing modalities. Further improvement to those two models can be done with enough funding and additional research time. An algorithm is developed for computing the *true* gray levels of an object of interest for the luggage inspection problem. This algorithm uses the overlap models and concepts like *textile* and *solid* objects in performing its analysis. The *true* gray level computation is focused on the transmission modalities. Once the scatter overlap models are refined, they can be easily added to the algorithm for computing *true* gray levels in those scatter modalities.